FIELD EVALUATION OF NDT DEVICES FOR DELAMINATION DETECTION OF HMA AIRPORT PAVEMENTS

Manuel Celaya, Ph.D. and Soheil Nazarian, Ph.D., PE

The University of Texas at El Paso (UTEP)

Advanced Infrastructure Design (AID)

Introduction

Delamination in Hot Mix Asphalt

Delamination in Airport Pavements

NDT Methods for Delamination Detection

Controlled Study

Field Investigation on Two Intl. Airports

NDT Results

Conclusions and Recommendations

Delamination in Hot Mix Asphalt

Bonding between pavement layers is essential.

Poor bond usually manifests as slippage cracking.

Poor bond may develop into delamination or debonding, reducing serviceability and performance.

If delamination goes undetected, it can result in the peeling away of thin overlays from the surface.

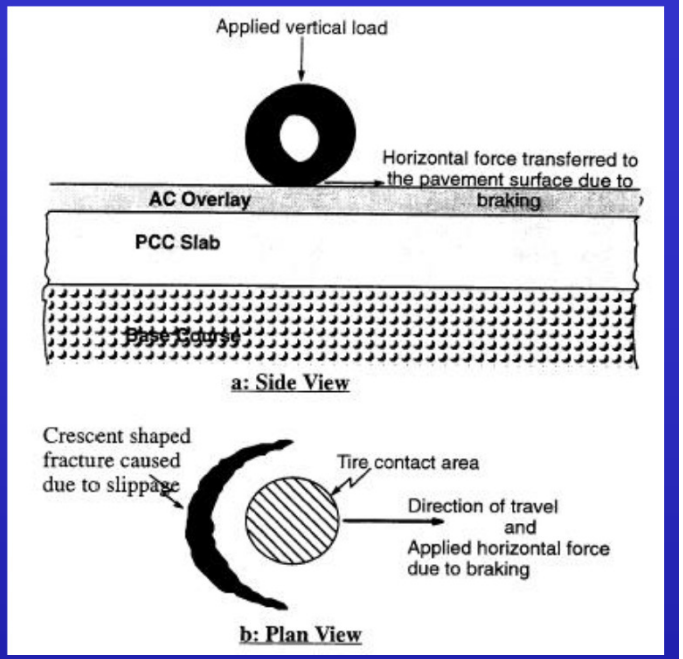

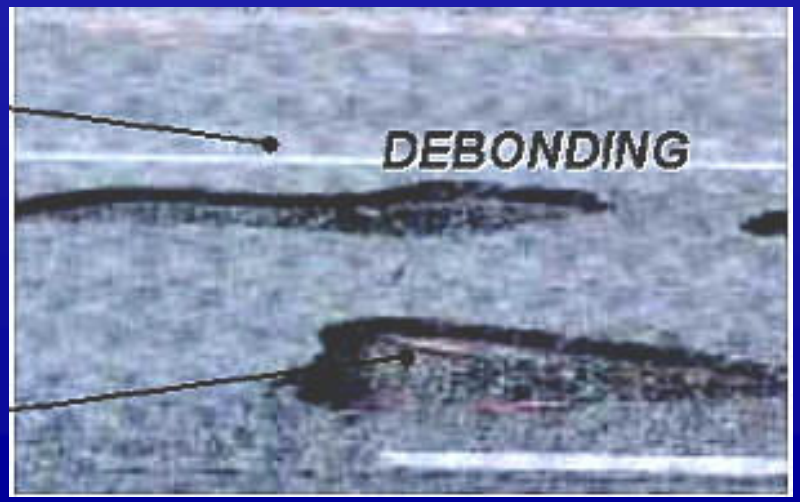

Delamination in Airport Pavements

Delamination is more severe on airfield pavements, due to higher traffic loads (aircrafts).

Situation is critical where airplanes brake and turn, or on areas under large horizontal load (slippage).

May develop into foreign object debris (FOD), leading to runway closures.

Slippage in Airports

FOD in Airports

FOD in Airports

NDT Methods for Delamination Detection

Most Promising NDT Methods:

Ground-coupled Penetrating Radar (GPR)

Portable Seismic Pavement Analyzer (PSPA)

Impulse Response (IR)

Falling Weight Deflectometer (FWD)

Thermography (Infrared Camera)

Others NDTs investigated but less successful: LWD, Stiffness Gauge, High Frequency Sweep, Ultrasound

Ground Penetrating Radar (GPR)

Base on the transmission of electromagnetic waves.

Reflections of these waves at interfaces used to determine their location or depth, and to determine the properties of material.

Used for:

- Measuring pavement thicknesses (ASTM D4748)
- Locate changes and anomalies
- Locate reinforcement and detect voids in concrete
- Locate moisture damage (stripping) in asphalt

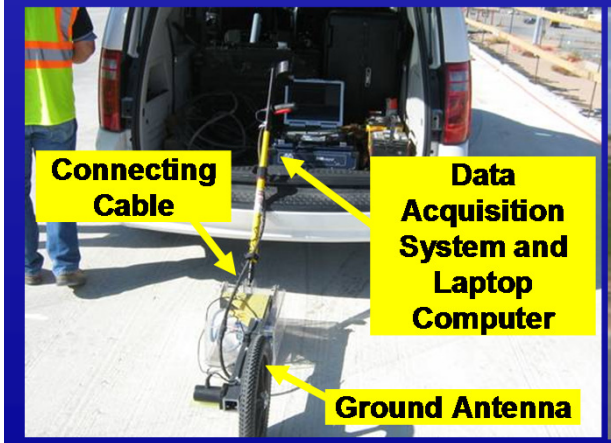

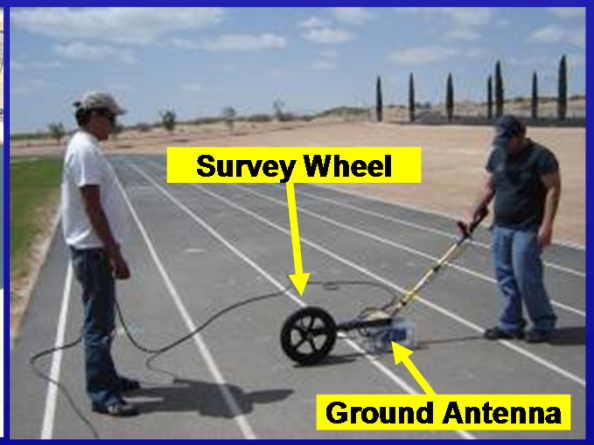

Ground-coupled (GPR)

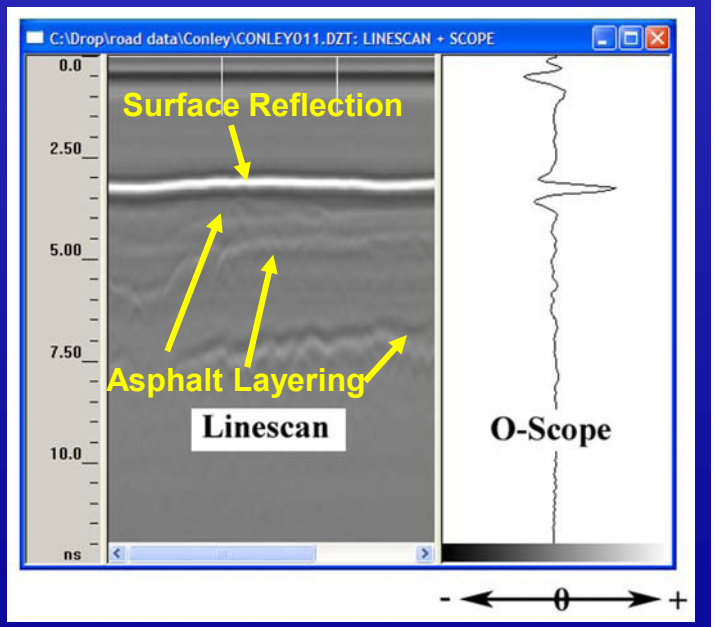

Typical GPR Scan

Portable Seismic Pavement Analyzer (PSPA)

High-frequency pulses are generated by the source and propagate through the testing material, reflecting at interfaces.

Modulus of top layer is calculated without an inversion algorithm (USW Method).

The Dispersion Curve (variation of velocity /modulus vs. wavelength/depth) is obtained using signal processing.

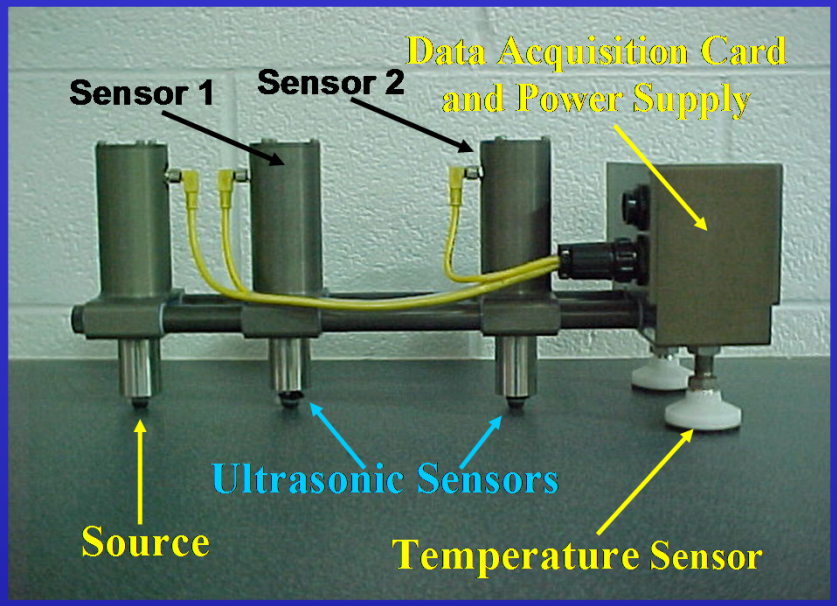

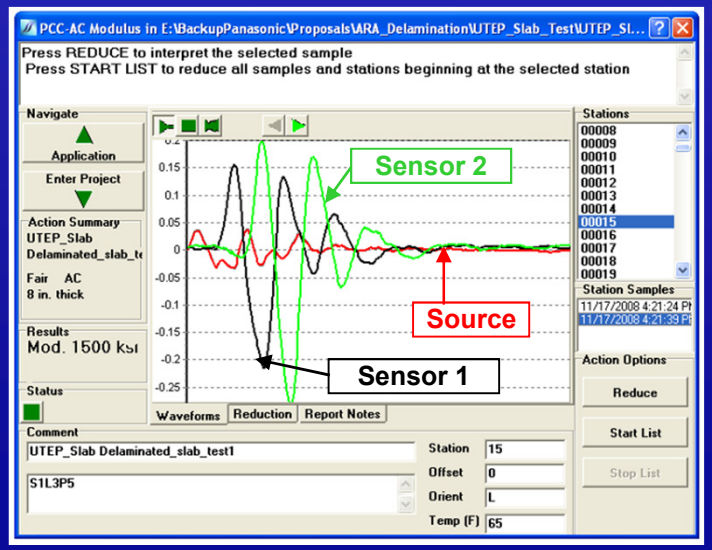

Time Records

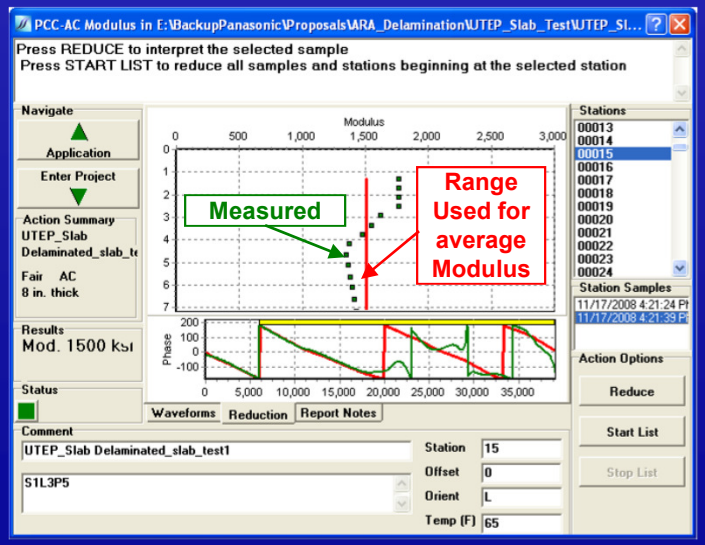

Dispersion Curve

Impulse Response (IR)

An impulsive loading is applied to the pavement surface with an instrumented hammer.

The vertical deformation of the pavement is measured with a geophone.

The ratio between the load cell and geophone amplitudes or the frequency responses using a Fast-Fourier Transform (FFT) is calculated.

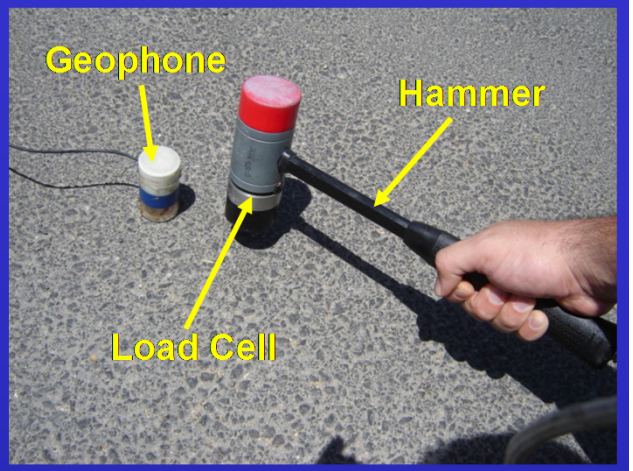

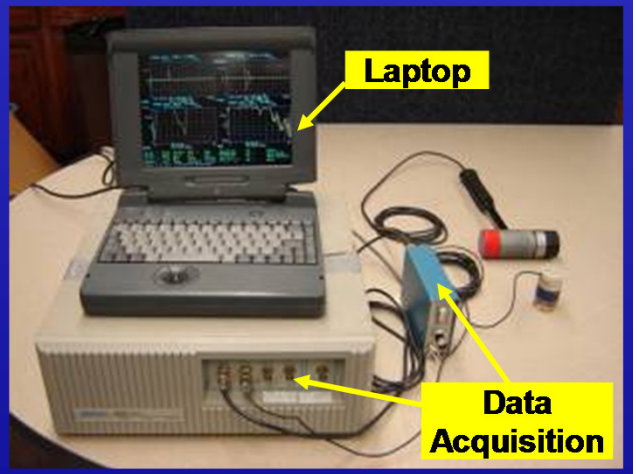

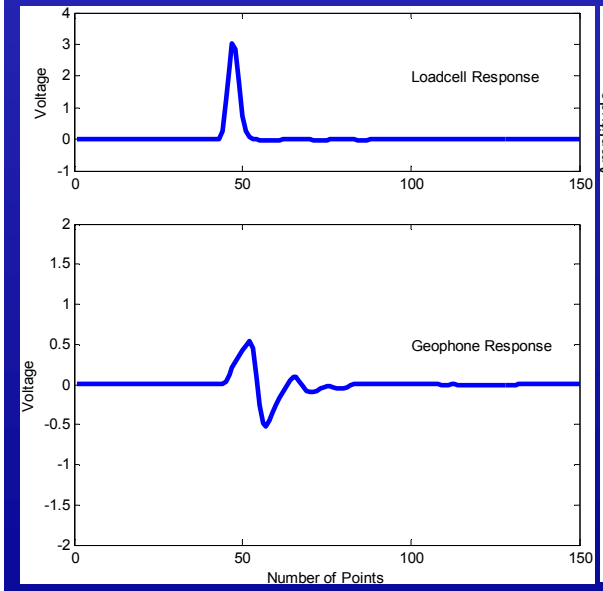

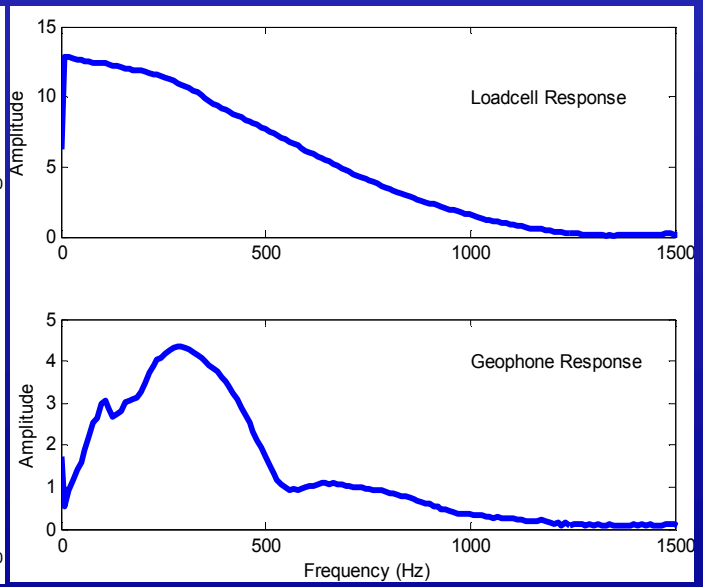

Time Records **Frequency Response**

Thermography: Infrared Camera

Infrared Thermography measures temperature distributions across the surface of the pavement.

Used to detect the presence of shallow subsurface flaws in HMA.

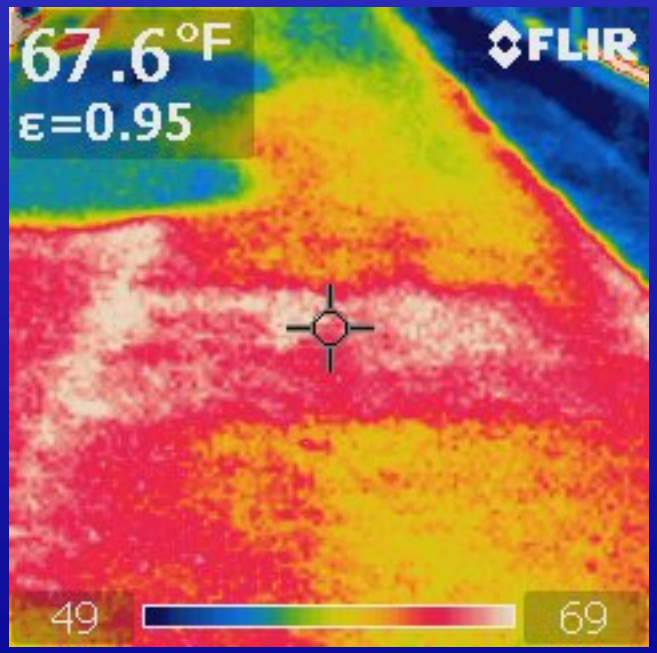

Infrared Image

Falling Weight Deflectometer (FWD)

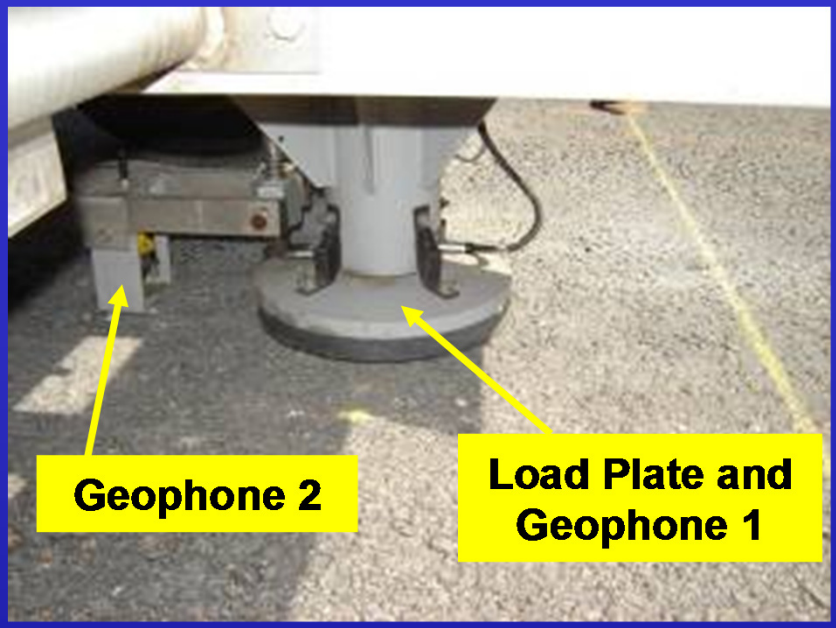

Impact loading mechanism and a set of seven geophones to measure vertical surface displacements. The entire system is trailer mounted.

The loading device is a 12 in. diameter load plate. An equivalent loads of 6,000 lbs was used.

First Geophone under the load plate. Other geophones at 1 ft interval.

Deflections of the first geophone and backcalculated modulus were used in this study.

Controlled Study

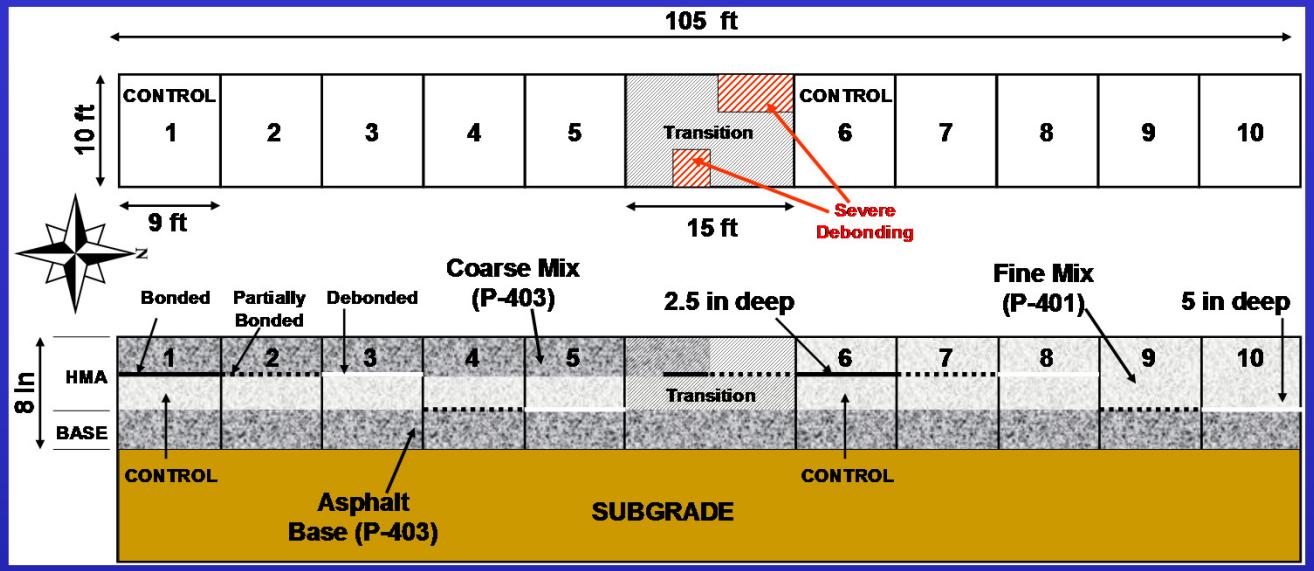

- 11 Different Sections constructed.
- Two mixes: Fine (P-401) and Coarse (P-403)
- Three levels of bonding between HMA: bonded, partially-bonded and debonded.
- In addition, severe debonding was reproduced.
- Two depths of debonding: shallow (2.5 in.) and deep (5 in.).
- Different extents of delamination.

Controlled Study

Selection of debonding agents based on laboratory tests (direct shear).

Each Section was 10x9 ft.

Delaminations of 4x9, 2x2, 1x1 and 0.5x0.5 ft were placed.

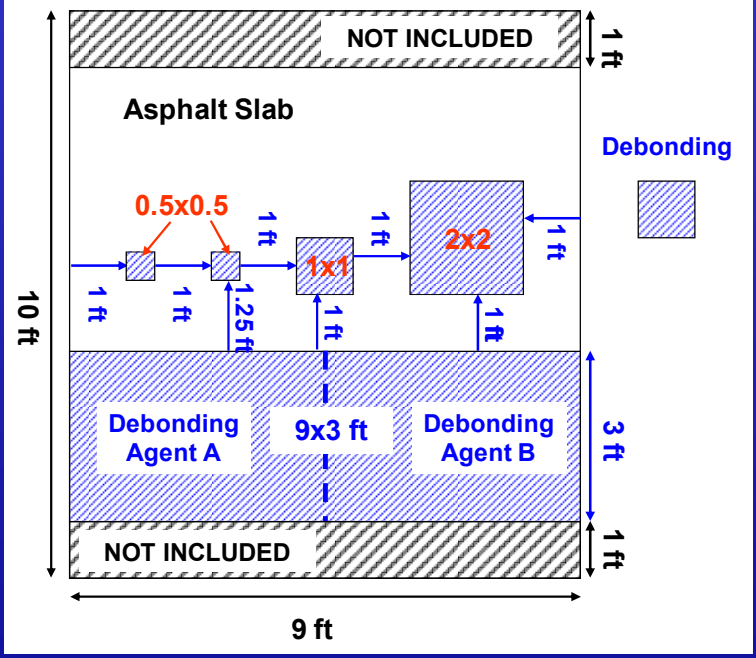

Typical Section Layout

Section	Surface Mix	Designation	Debonding Agent				
			Tack Coat	Grease	Clay Slurry	Talcum Powder	Paper with Oil
1	Coarse Mix	Control	√				
2		Shallow Partially-Debonded		√	√		
3		Shallow Fully-Debonded				√*	√
4		Deep Partially-Debonded		√	√		
5		Deep Fully-Debonded				√*	√
6	Fine Mix	Control	√				
7		Shallow Partially-Debonded		√	√		
8		Shallow Fully-Debonded				√*	√
9		Deep Partially-Debonded		√	√		
10		Deep Fully-Debonded				√*	√

** Partially-Debonded*

Debonding Agents Used

Test Setup

A grid of 10x10 points was selected for PSPA, IR and Infrared.

10 Lines were evaluated with GPR.

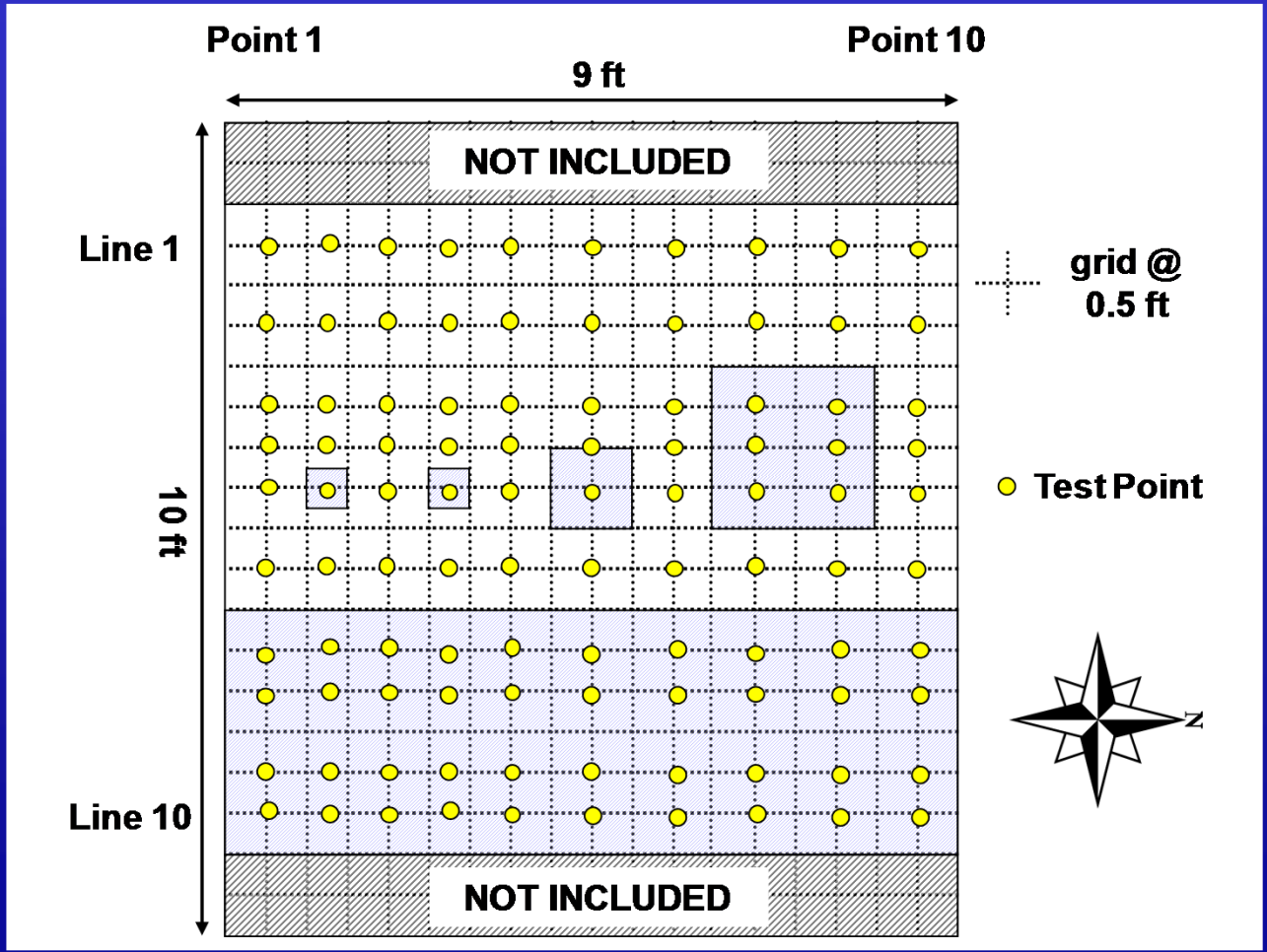

Conclusions from Controlled Study

- Impulse Response (best for fully debonded, especially deep)
  - detected 59% of debonded areas.
- GPR (best for severe debonding with moisture)
  - detected 33% of debonded areas.
- Ultrasonic Surface Waves (best for shallow partial or full debonding)
  - The USW method (PSPA) detected 53% of debonded areas.
- Thermography was not as successful as reported in the literature.
- FWD detected 46% of debonded areas, best during cold weather testing.
- The IR, FWD and USW methods require temperature adjustments.

Field Evaluation of NDT Methods

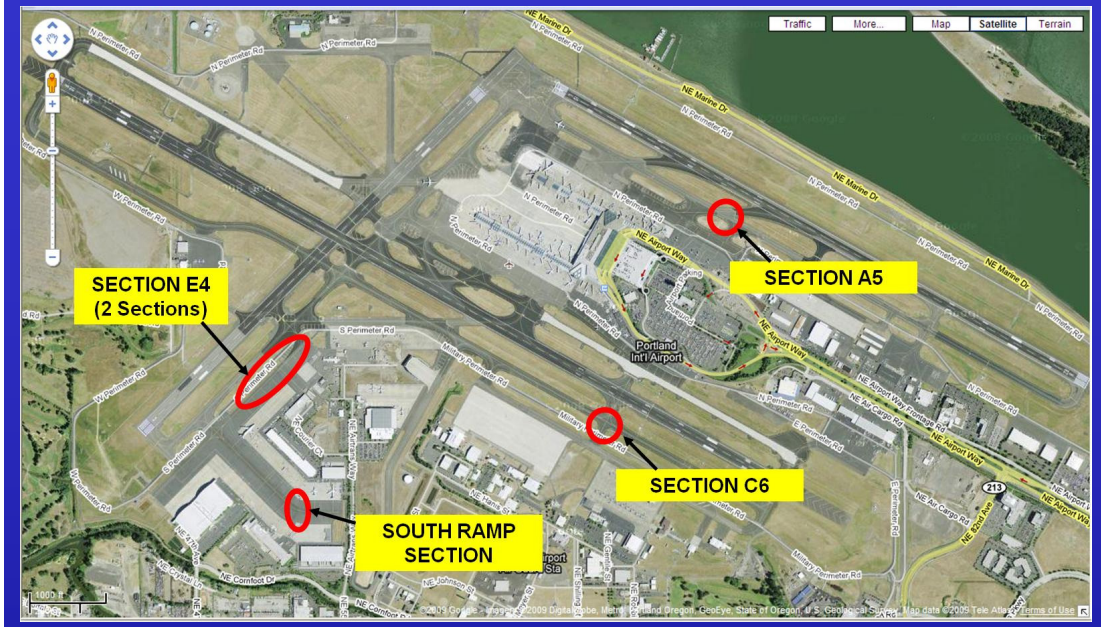

Portland International Airport (PDX)

Boston Logan International Airport (BOS)

- 5 Sections Investigated
- PSPA, GPR, Infrared, impulse Response and FWD
- Validation coring

- 2 Sections Investigated
- PSPA, GPR, and impulse Response
- Validation coring

PDX Airport Test Layout

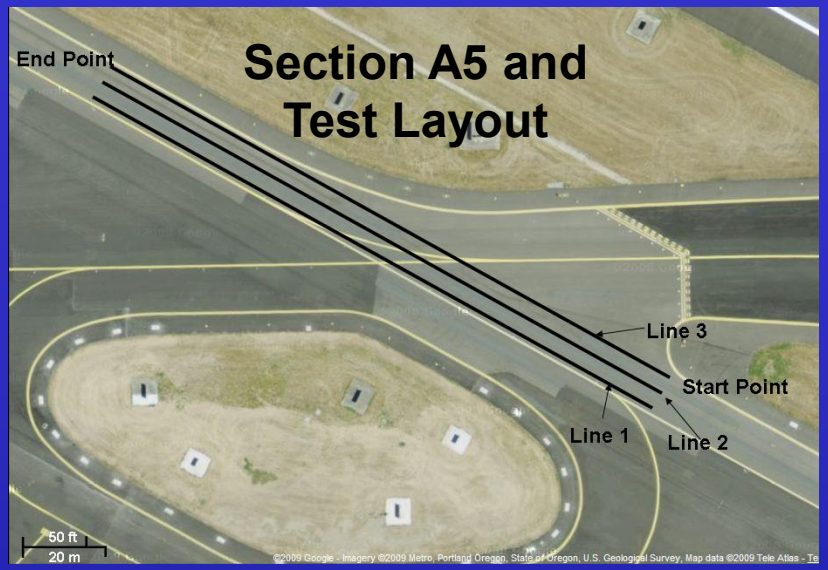

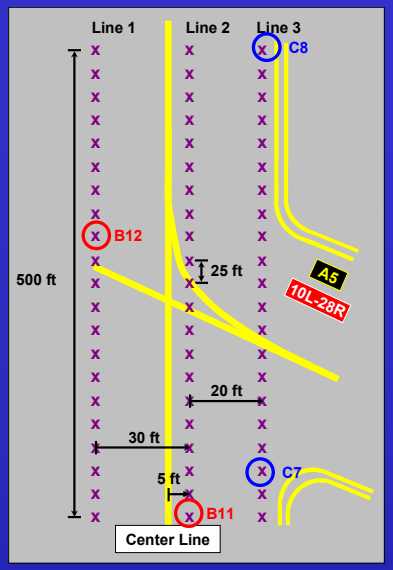

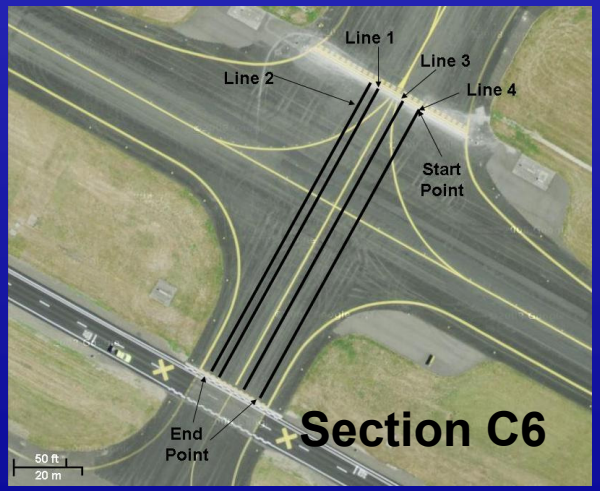

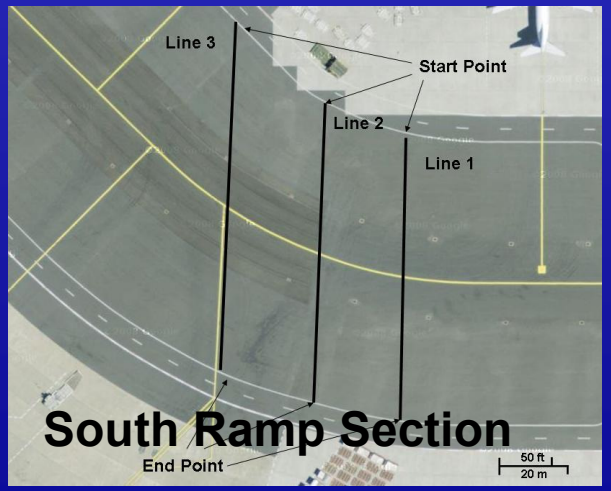

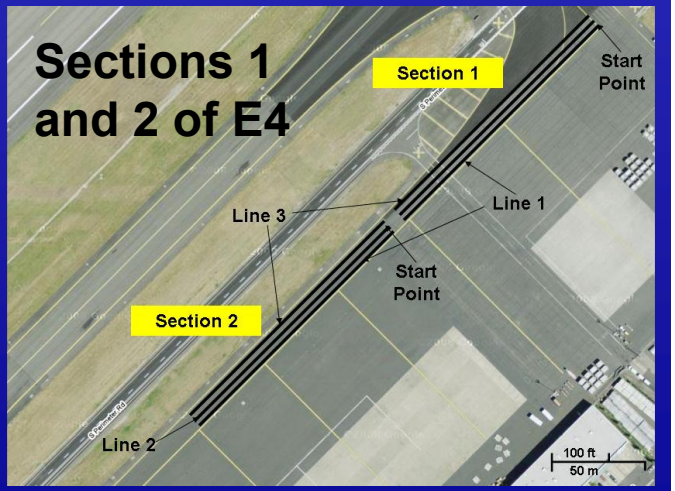

5 Sections Investigated

PDX. NDT Methods Used

GPR

FWD

Impulse Response

PSPA

Coring

Coring

PDX Summary Results (Sect. A5)

GPR

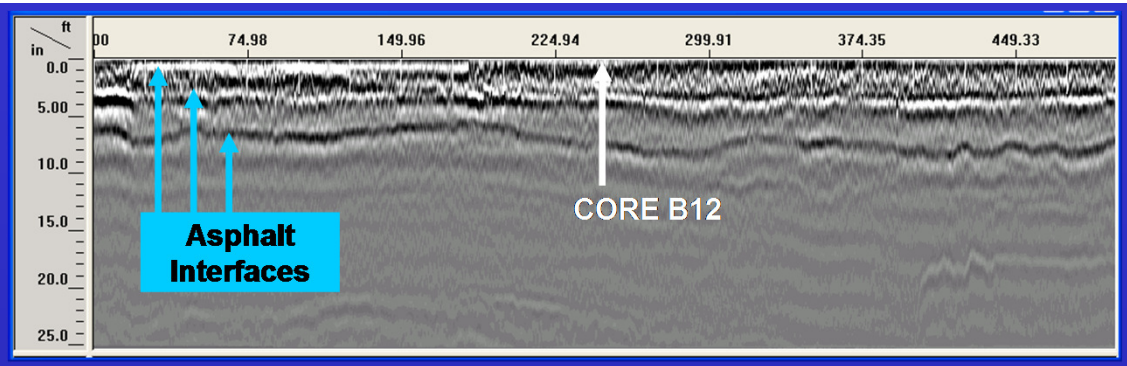

PSPA

	Distance from Start Point (ft)																				
	0	25	50	75	100	125	150	175	200	225	250	275	300	325	350	375	400	425	450	475	481	500
Line 1	1905	1715	2017	1678	1785	1669	2082	1567	1984	1868	2116	1748	1857	1864	1804	1755	1766	1819	2014	1984	N/A	2026
Line 2	2432	2105	1879	2028	2143	2483	1891	1748	2112	2032	2171	1876	2034	1350	2330	1651	2372	1350	2330	2086	2211	1318
Line 3	1120	1220	1150	1383	1960	1730	1210	1319	1439	1049	1558	1665	1772	1314	1688	1879	1765	2063	1714	1627	N/A	1259

Impulse Response

	Distance from Start Point (ft)																				
	0	25	50	75	100	125	150	175	200	225	250	275	300	325	350	375	400	425	450	475	481	500
Line 1	6.8	12.3	11.0	10.0	7.6	9.5	10.9	11.1	9.8	6.9	9.1	5.7	9.3	10.7	6.4	6.6	4.6	5.5	5.5	5.5	N/A	6.1
Line 2	9.8	8.7	9.0	11.6	6.7	11.4	12.5	8.1	7.5	7.7	9.0	5.9	11.0	12.1	13.9	6.3	7.7	3.9	6.5	7.4	6.8	8.4
Line 3	2.6	2.0	2.0	2.2	7.4	9.7	8.4	4.1	5.3	6.0	3.5	8.4	6.0	9.9	5.0	4.1	4.2	4.2	3.5	3.4	N/A	4.0

FWD

	Distance from Start (ft)										
	0	50	100	150	200	250	300	350	400	450	500
Line 1	10.2	9.4	9.5	9.5	8.8	8.9	9.2	9.9	9.6	13.6	14.4
Line 2	11.3	10.3	8.9	8.6	8.7	9.7	8.8	7.2	9.7	13.2	12.7
Line 3	20.9	29.0	9.9	10.4	9.7	8.4	9.5	15.5	16.3	16.1	15.9

PDX Coring Results

Section A5

Section C6

South Ramp

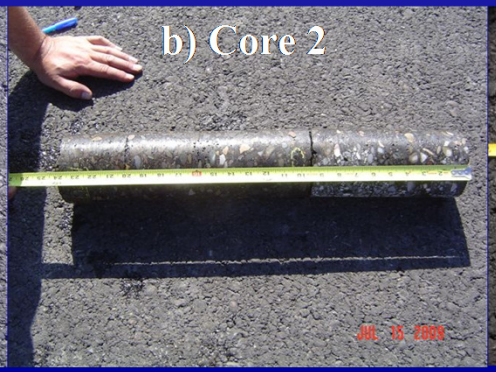

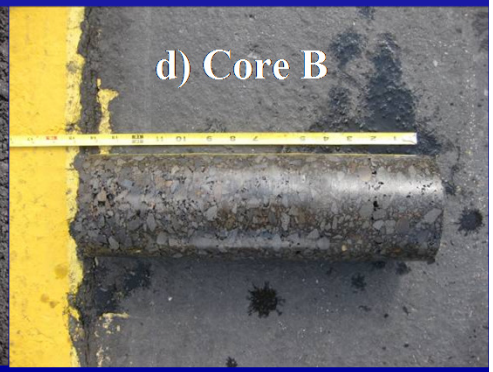

Sections 1 and 2 of E4

PDX Comparison of NDT with Cores

Core #	Location	GPR	PSPA	IR	FWD	Condition/Comments
B11	Line 2 @0 ft	Intact	Intact	Intact	Intact	Intact
B12	Line 1 @250 ft	Suspect	Intact	Intact	Intact	Intact
C7	Line 3 @0 ft	Suspect	Damaged	Damaged	Damaged	Low quality HMA, Core broken at 9.5 in.
C8	Line 3 @500 ft	Intact	Damaged	Damaged	Damaged	Low quality HMA, Intact
C10	L1 @160 ft from start	Intact	Damaged	Damaged	Intact	Stripping between top and middle layer
C3	L1 @100 ft from start	Intact	Intact	Marginal	Intact	Intact.
C4	L1 @140 ft from start	Intact	Intact	Damaged	Damaged	Some stripping at 9 in.
C5	L1 @160 ft from start	Intact	Intact	Damaged	Damaged	Intact
C6	L3 @280 ft from start	Damaged	Damaged	Damaged	Damaged	Severe stripping between each lift
Core 1	L2 @ 150 ft from start	Intact	Damaged	Marginal	Intact	Intact
Core 2	L3 @ 375 ft from start	Damaged	Damaged	Damaged	Damaged	Intact/Low quality HMA
Core A	L1 @0 ft from start	Damaged	Damaged	Damaged	Damaged	Intact/Low quality HMA
Core B	L1 @50 ft from start	Damaged	Intact	Intact	Intact	Intact Core. Sample length 14½“

BOS Test Layout

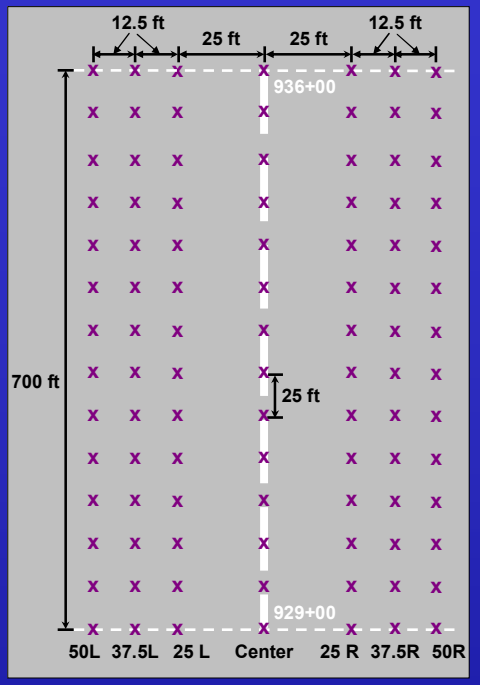

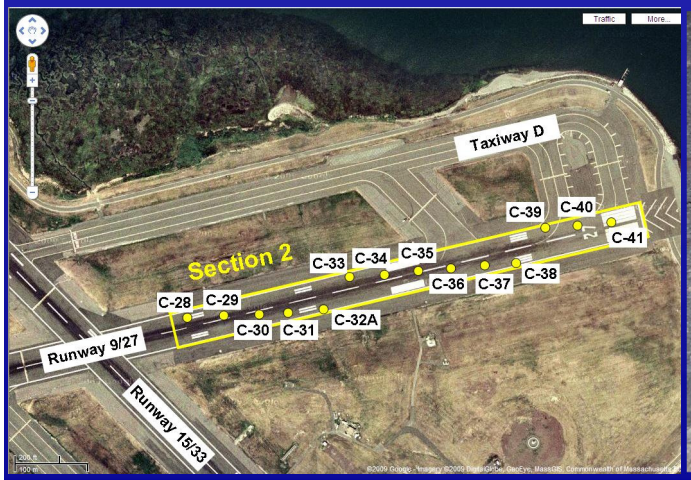

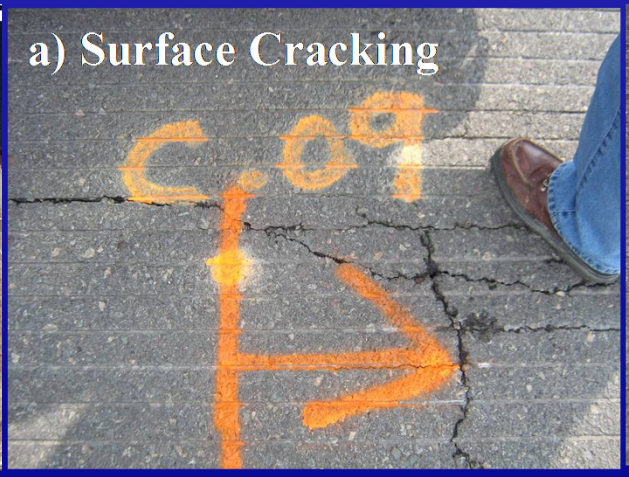

BOS . NDT Methods Used

Impulse Response and PSPA

GPR

Ongoing Construction

BOSTON Summary Results

GPR

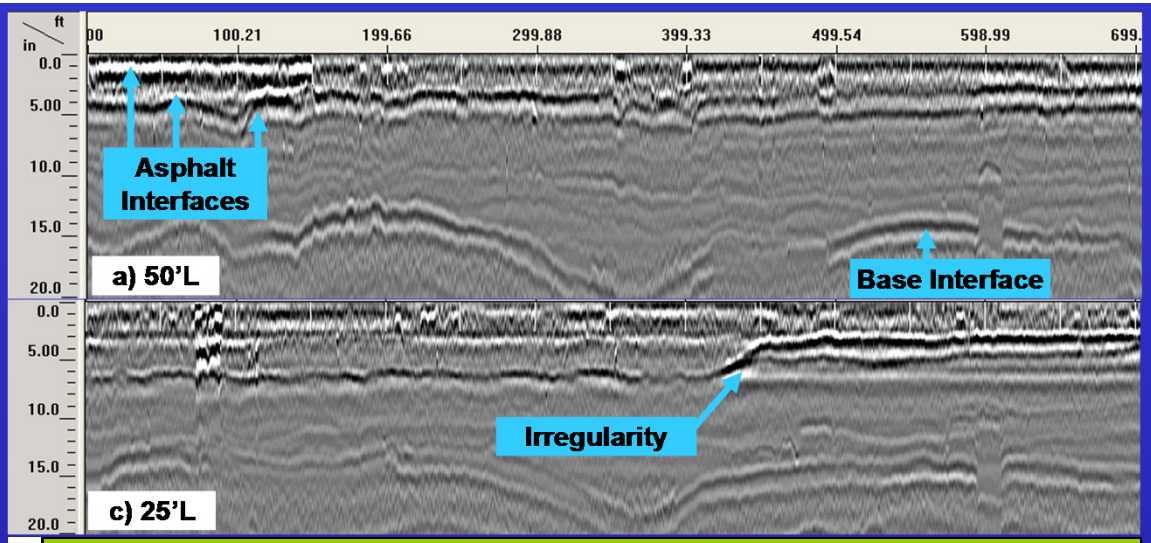

PSPA

	Test Location																												
	92900	92925	92950	92975	93000	93025	93050	93075	93100	93125	93150	93175	93200	93225	93250	93275	93300	93325	93350	93375	93400	93425	93450	93475	93500	93525	93550	93575	93600
L50	807	1,021	930	1,072	790	1,798	1,383	1,607	787	1,614	1,384	1,792	1,712	1,873	1,815	1,655	1,059	1,838	1,751	1,664	1,896	1,908	1,942	1,850	816	2,287	2,213	1,941	1,998
L37.5	799	1,188	556	1,082	823	635	1,150	997	1,601	1,110	1,998	897	814	931	601	554	548	2,036	2,129	2,129	1,536	2,187	2,226	1,991	2,109	2,179	2,321	2,036	1,937
L25	963	790	823	1,407	1,007	926	963	1,059	867	1,016	847	921	1,003	839	1,141	891	911	771	832	882	902	659	971	1,219	1,129	1,030	1,080	991	1,055
0	402	780	329	385	642	393	298	436	338	549	597	402	680	613	289	565	683	596	247	887	1,259	974	414	358	277	398	277	256	305
R25	690	975	259	594	549	716	581	489	553	654	737	655	682	1,178	609	573	524	425	488	272	542	359	553	569	554	418	375	368	337
R37.5	1,815	1,334	1,539	1,497	1,456	376	2,423	2,024	1,269	1,018	2,007	1,934	1,726	352	701	1,402	415	1,084	1,564	930	1,634	1,778	1,634	1,426	2,075	1,964	1,557	1,425	1,181
R50	1,464	1,360	1,256	1,194	1,659	1,738	1,615	1,677	1,811	1,331	1,180	1,319	1,319	2,089	1,416	1,978	1,402	2,088	1,130	2,432	1,735	2,235	2,012	2,012	1,554	2,099	1,669	2,124	1,931

Impulse Response

	Test Location																												
	92900	92925	92950	92975	93000	93025	93050	93075	93100	93125	93150	93175	93200	93225	93250	93275	93300	93325	93350	93375	93400	93425	93450	93475	93500	93525	93550	93575	93600
L50	6.21	3.79	1.96	2.49	2.70	3.65	4.82	5.71	5.68	7.49	7.37	4.58	6.76	4.87	5.77	5.46	7.44	5.42	4.66	6.23	8.38	6.44	4.91	7.20	6.26	5.26	7.50	6.62	4.33
L37.5	4.66	5.15	4.36	3.28	6.04	3.46	6.57	6.80	9.56	9.08	6.10	4.42	3.51	5.21	4.10	3.28	1.97	5.79	5.19	5.70	6.08	6.53	6.24	4.97	5.52	4.50	6.09	6.17	6.89
L25	1.13	2.77	2.89	1.32	1.87	1.75	2.81	1.83	2.20	1.54	2.54	3.24	3.69	4.17	2.84	3.41	3.59	2.76	3.38	3.06	7.14	2.21	4.22	8.27	4.53	6.24	6.75	3.96	4.16
0	0.56	0.91	1.87	1.49	0.96	0.44	0.98	0.51	0.69	0.71	0.59	0.87	0.89	0.20	0.41	0.50	0.84	0.49	0.21	0.47	0.36	0.33	0.37	1.25	0.19	0.40	0.14	0.44	0.42
R25	0.87	0.60	0.71	0.52	0.63	1.03	0.34	1.78	0.55	0.41	1.03	1.57	2.28	1.83	1.01	4.04	0.94	0.36	0.81	0.62	0.60	0.41	1.48	0.74	0.68	0.58	0.42	0.45	1.32
R37.5	5.01	4.36	1.71	1.32	0.72	0.84	2.18	2.26	2.10	3.10	4.72	5.39	1.73	1.46	1.37	2.11	2.64	3.31	2.20	3.94	4.85	4.55	7.54	4.76	4.21	3.85	4.34	6.71	5.48
R50	2.30	3.49	3.17	3.92	0.89	1.93	3.25	6.17	2.48	3.88	2.67	3.44	2.74	5.50	4.26	7.26	2.90	4.80	1.75	4.50	2.51	4.47	4.22	3.92	9.15	2.99	2.65	5.03	6.22

BOS Coring Results

Section 1

Section 2

BOS Comparison of NDT with Cores

Core #	Location	GPR	PSPA	IR	Condition/Comments
C-15	929+50 @40'R	Intact	Intact	Intact	Intact
C-16	931+00 @60'R	Damaged	N/A	N/A	Intact
C-17	932+50 @10'L	Damaged	Marginal	Intact	Debonding at 6 in.
C-18	934+00 @10'R	Damaged	Damaged	Damaged	Debonding at 3 in.
C-19	935+50 @40'R	Damaged	N/A	N/A	Debonding at 7 in.
C-28	949+00 @40'L	N/A	Marginal	Intact	Intact
C-29	950+50 @10'L	N/A	Intact	Damaged	Intact
C-30	952+00 @10'R	N/A	Damaged	Damaged	Debonding at 6 in.
C-30A	952+05 @10'R	N/A	Marginal	Intact	Intact
C-31	953+50 @40'R	N/A	Intact	Intact	Intact
C-32A	954+95 @65'R	N/A	Intact	Intact	Intact
C-33	956+50 @60'L	N/A	Intact	Intact	Intact
C-34	958+00 @40'L	N/A	Intact	Intact	Intact
C-35A	959+50 @10'L	N/A	Damaged	Intact	Debonding at 7 in.
C-36	961+00 @10'R	N/A	Intact	Intact	Intact
C-37	962+50 @40'R	N/A	Intact	Intact	Core rig malfunctioned at core had to be stopped at 9 ½".
C-38	964+00 @60'R	N/A	Intact	Marginal	Intact
C-39	965+50 @60'L	N/A	Marginal	Marginal	Debonding at 4 in.
C-40	967+00 @40'L	N/A	Marginal	Damaged	Debonding at 4 in.

Conclusions from Field Investigation

- For the most part similar conclusions from the controlled study.
- Testing of airports revealed many complexities.
- In general, all methods located damaged areas with a probability >50%.
- The higher predictive power at PDX was attributed to severely debonded and stripped locations that were absent at BOS.
- Intact points not identified as intact was about 43%. Cores from these points were not debonded, but exhibited micro-cracking or lower quality HMA
- Mechanical NDT methods (PSPA, IR and FWD) detected shallow severely debonded areas with reasonable certainty.
- GPR results seemed to be ambiguous.
- For complex pavement sections, FWD is less effective.
- Delineation of low-quality HMA from debonding is difficult from all mechanical NDTs. More sophisticated data processing should be considered

Questions?

Acknowledgments

The University of Texas at El Paso (UTEP)

Advanced Infrastructure Design (AID)

NDT Results on Controlled Study

GPR Results

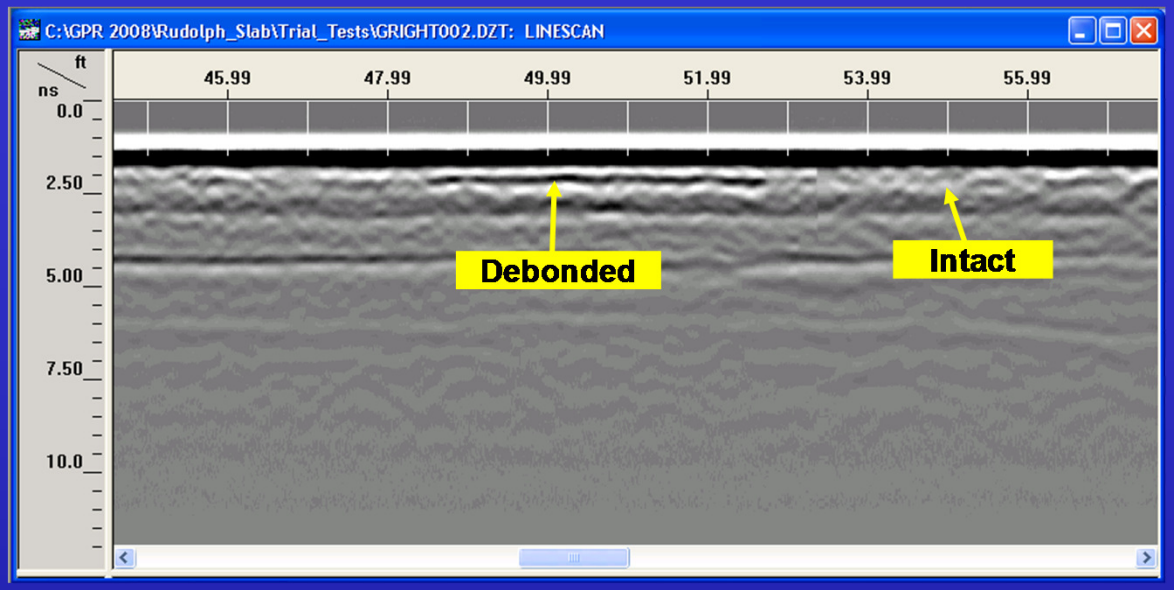

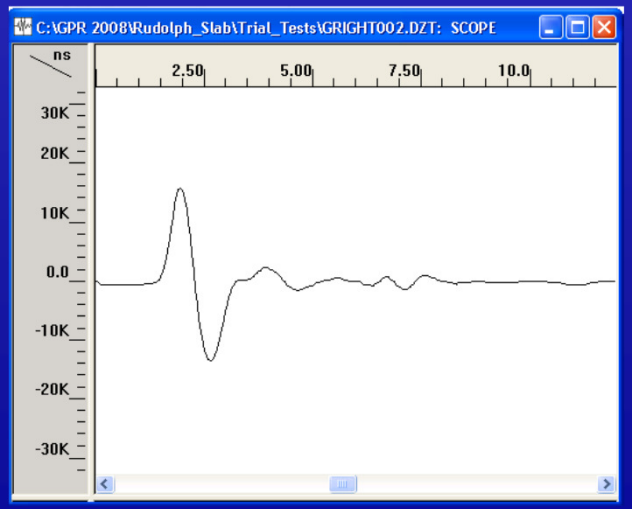

Intact

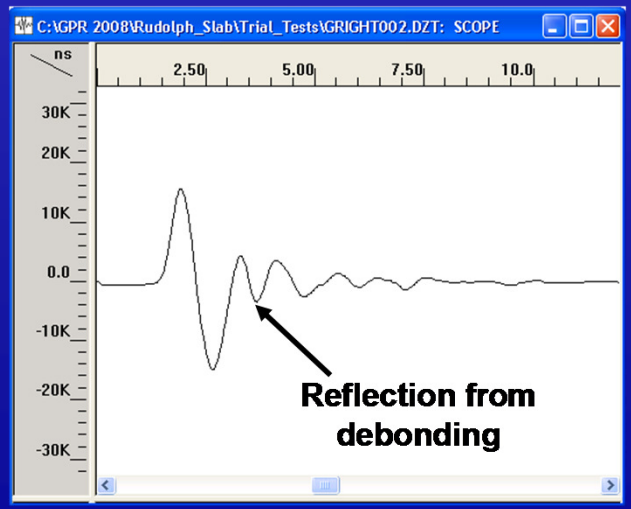

Severe Debonded

GPR Results

GPR detected the severely debonded area within the transition zone and some debonded areas primarily on talcum powder or clay perhaps because of the significant contrasts in their dielectric constants and HMA.

GPR may be most suitable when the debonding is in severe stages or when moisture is present along the interface.

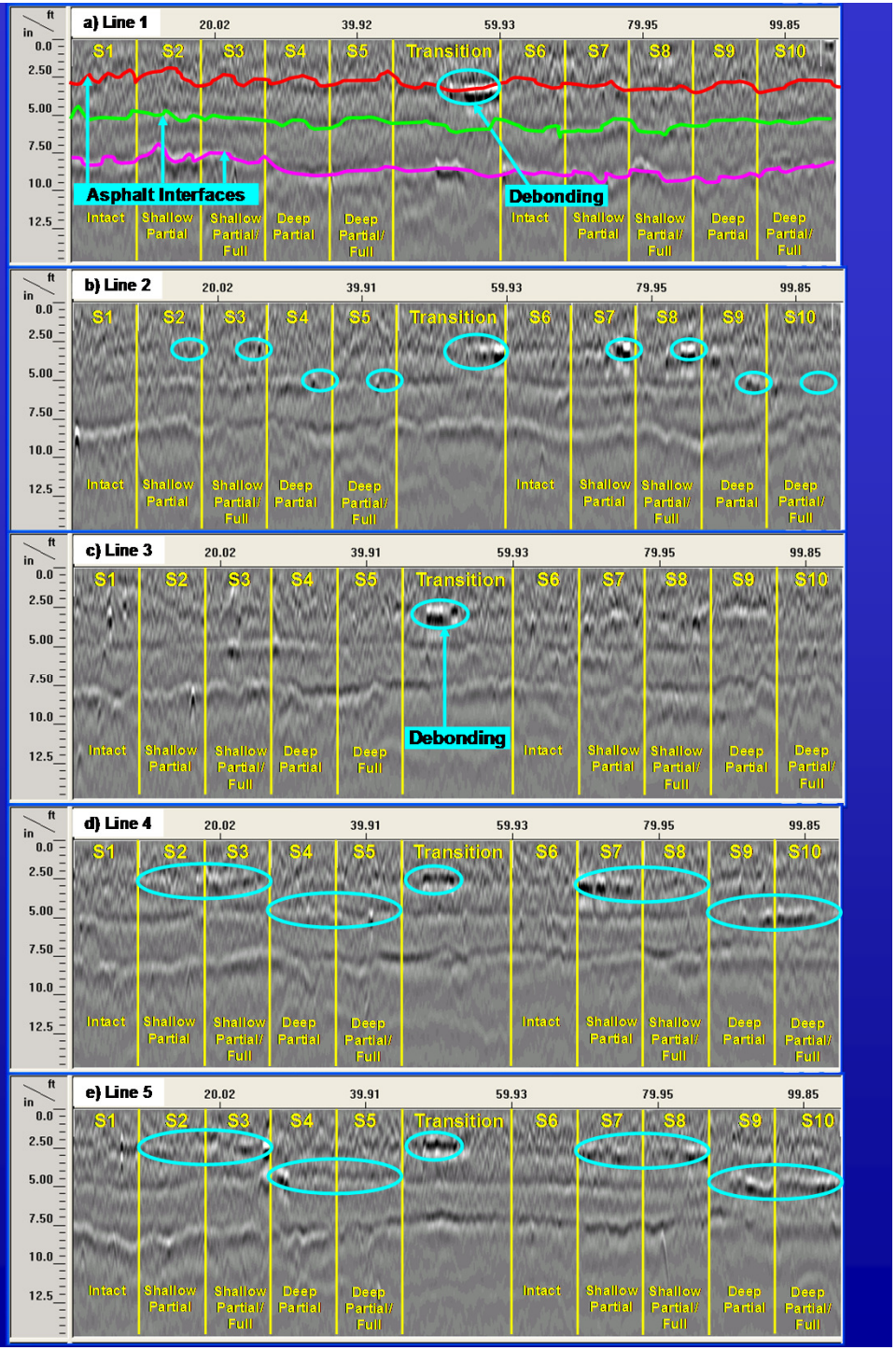

PSPA Results

Time Records

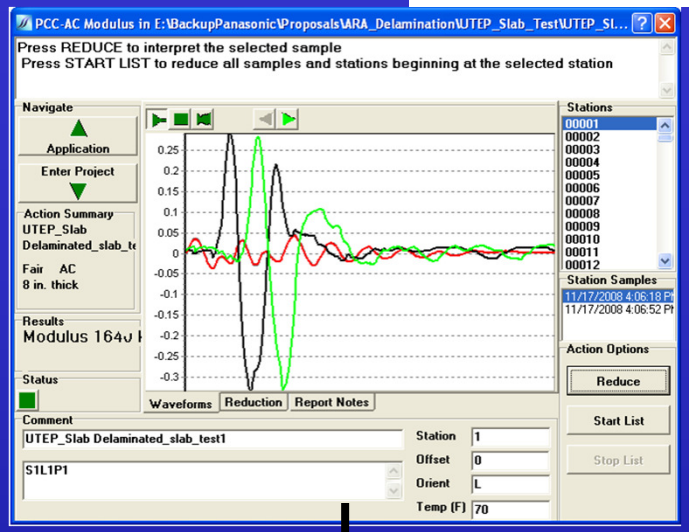

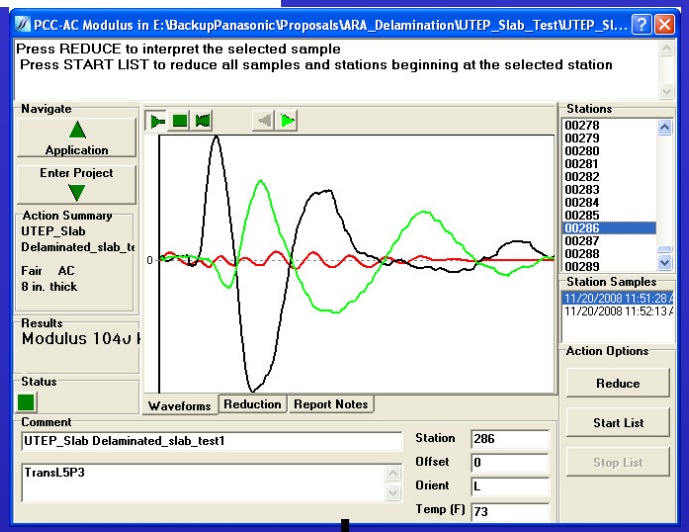

Dispersion Curves

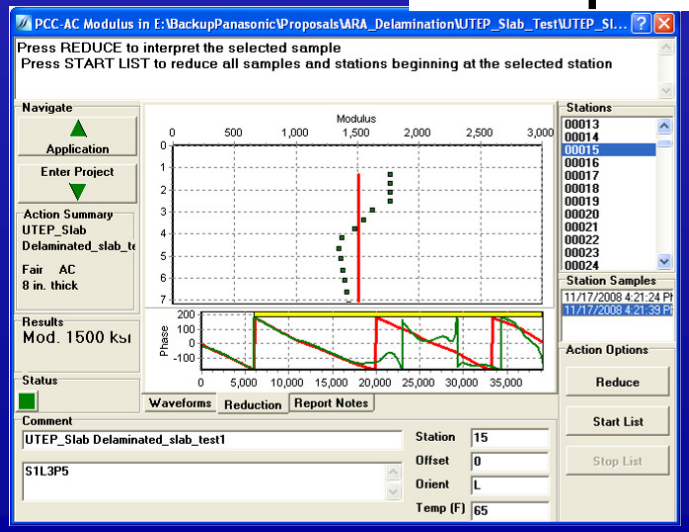

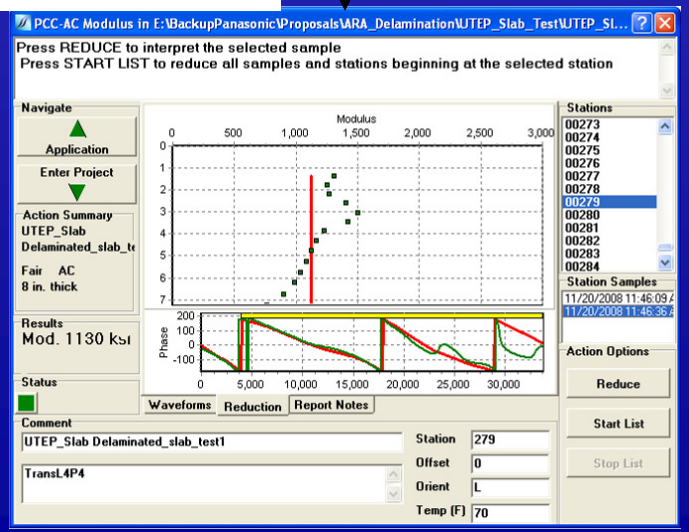

Intact

Severe Debonded

PSPA Results. Dispersion Curves

Reductions in modulus can be observed in most sections below depths of prepared debonding.

This demonstrates that the USW method might be able to identify delaminated areas reasonably well, especially the shallow ones.

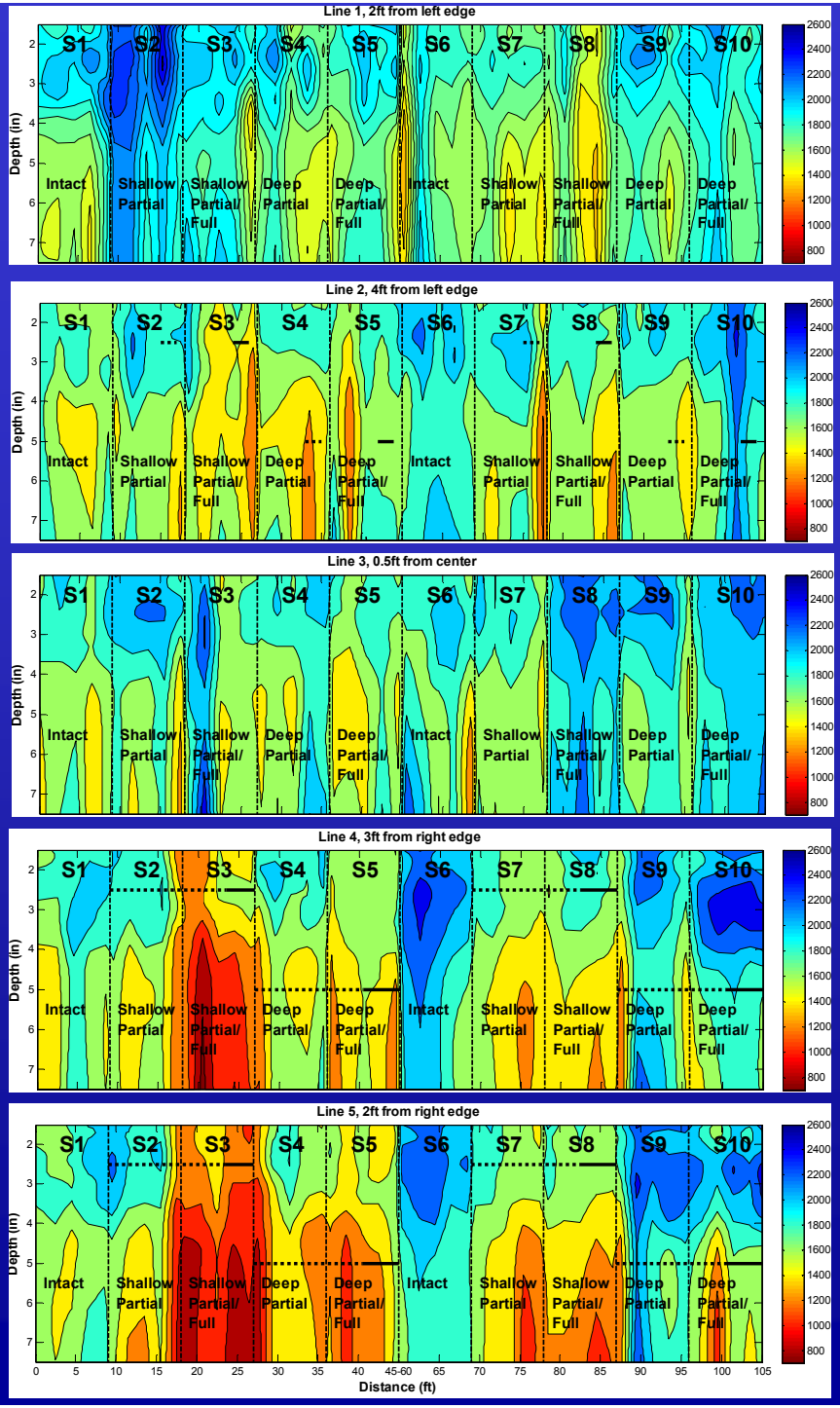

PSPA Results. Overall

Coarse Mix (P-403)

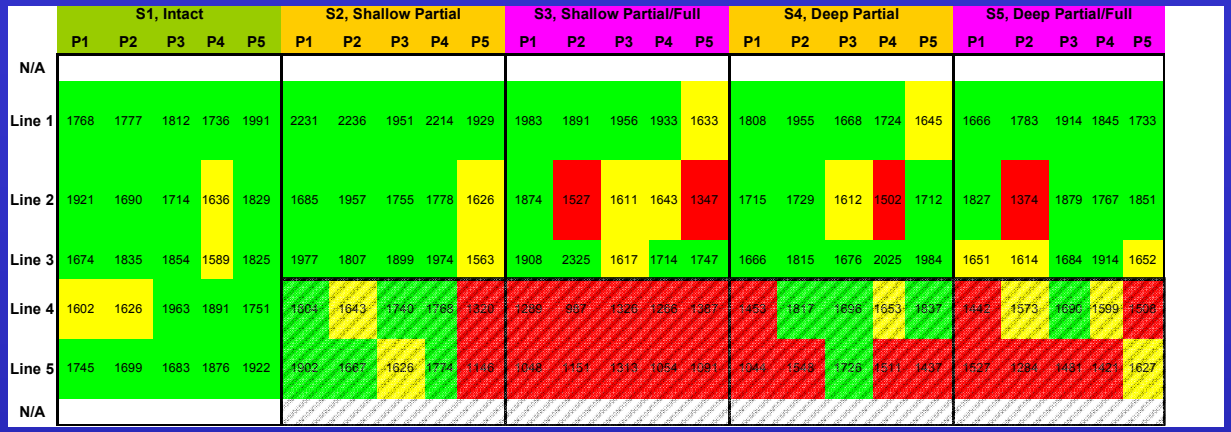

Fine Mix (P-401)

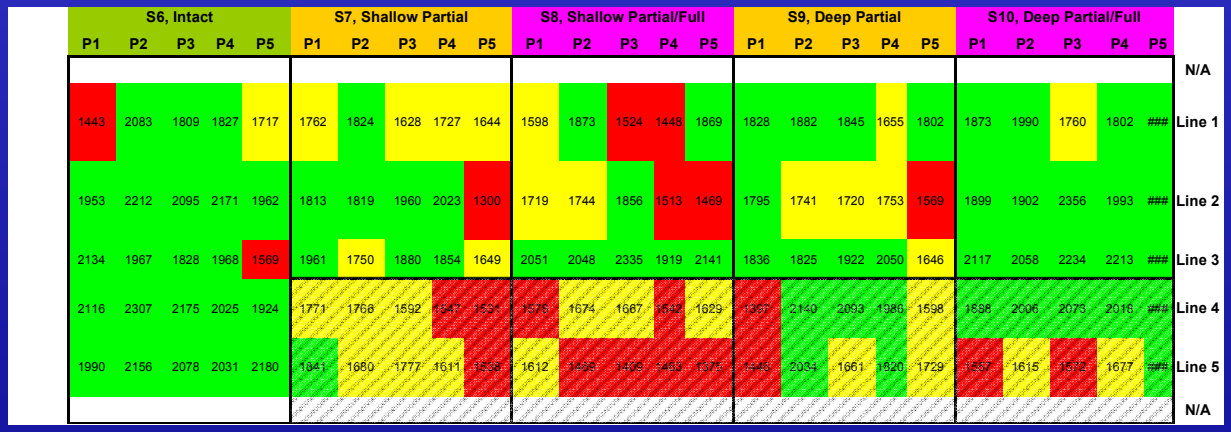

Average and standard deviation of control sections (1 and 6) used as reference

Color Code	Modulus Value	Interpretation
Green	$E > E_{control} - \sigma_{control}$	Measured modulus is similar or higher than modulus from control section
Yellow	$E_{control} - \sigma_{control} > E > E_{control} - 2\,\sigma_{control}$	Measured modulus is somewhat less than control modulus
Red	$E < E_{control} - 2\,\sigma_{control}$	Measured modulus is substantially less than control modulus

IR Results

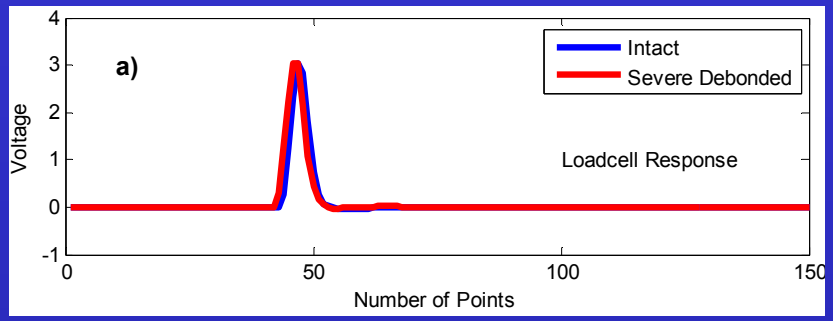

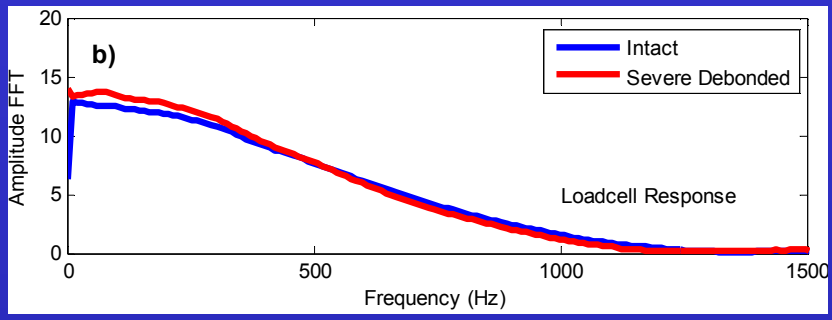

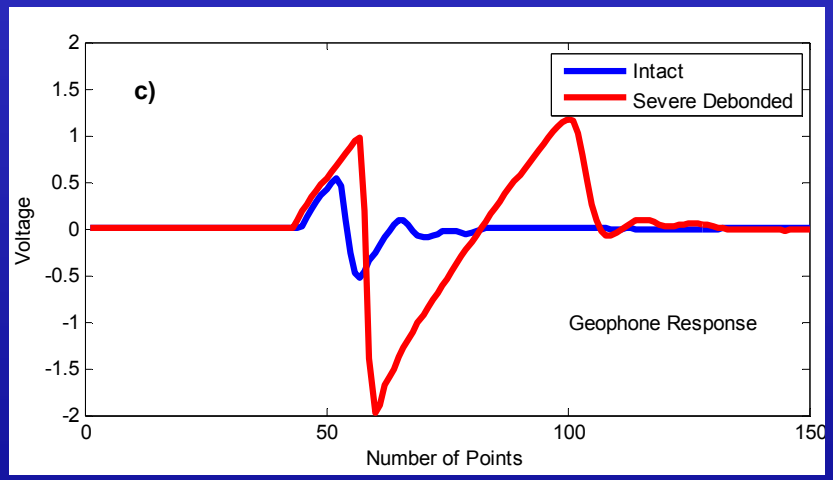

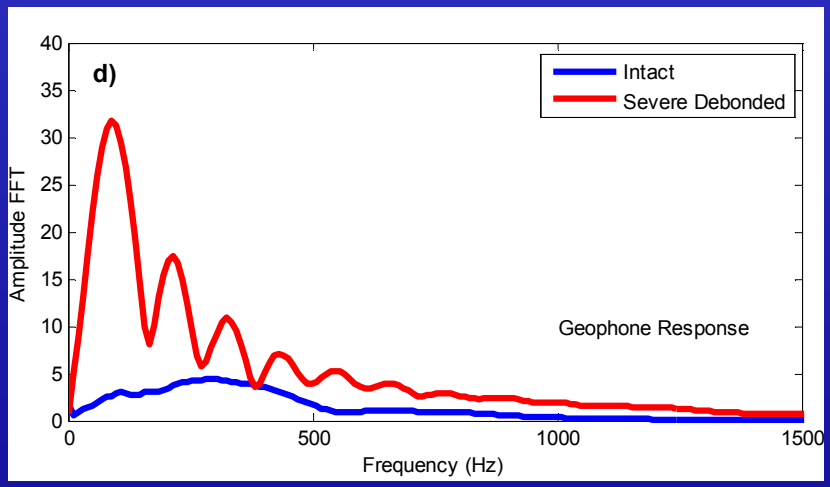

Time Records → **Frequency Response**

The ratio (load/displacement) of the maximum values of the FFT amplitudes (stiffness) used to compare the results

IR Results. Temperature Influence

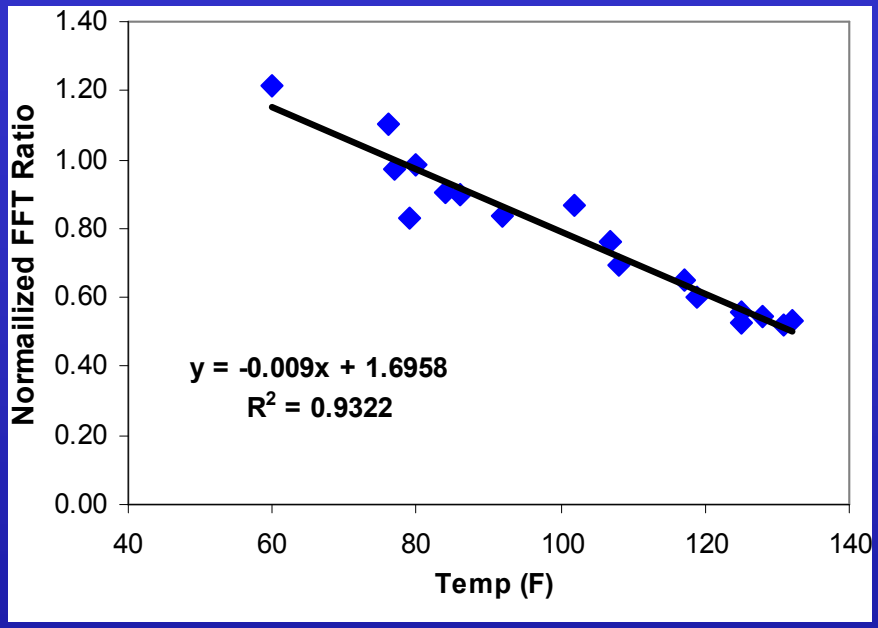

Coarse Mix (P-403)

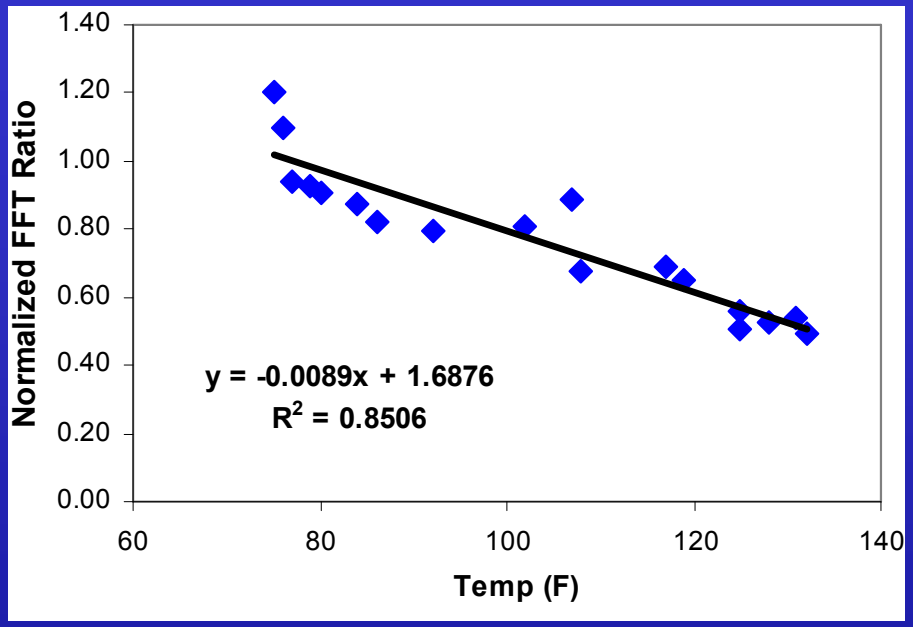

Fine Mix (P-401)

Temperature at the time of testing affects the outcome of this method

IR Results. Overall

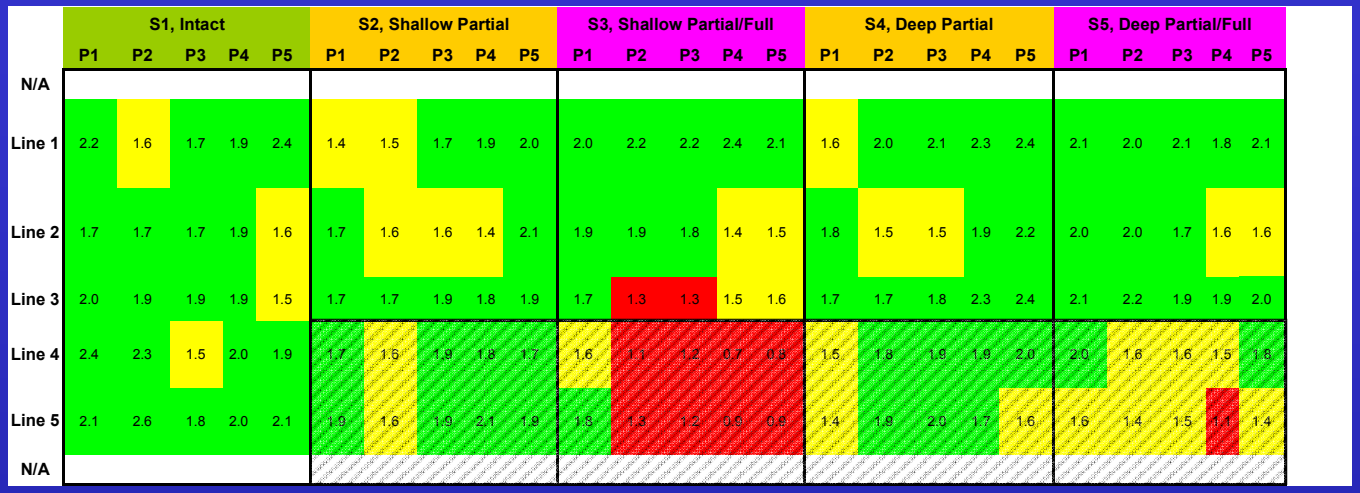

$E > E_{control} - \sigma_{control}$

$E_{control} - \sigma_{control} > E > E_{control} - 2*\sigma_{control}$

$E < E_{control} - 2*\sigma_{control}$

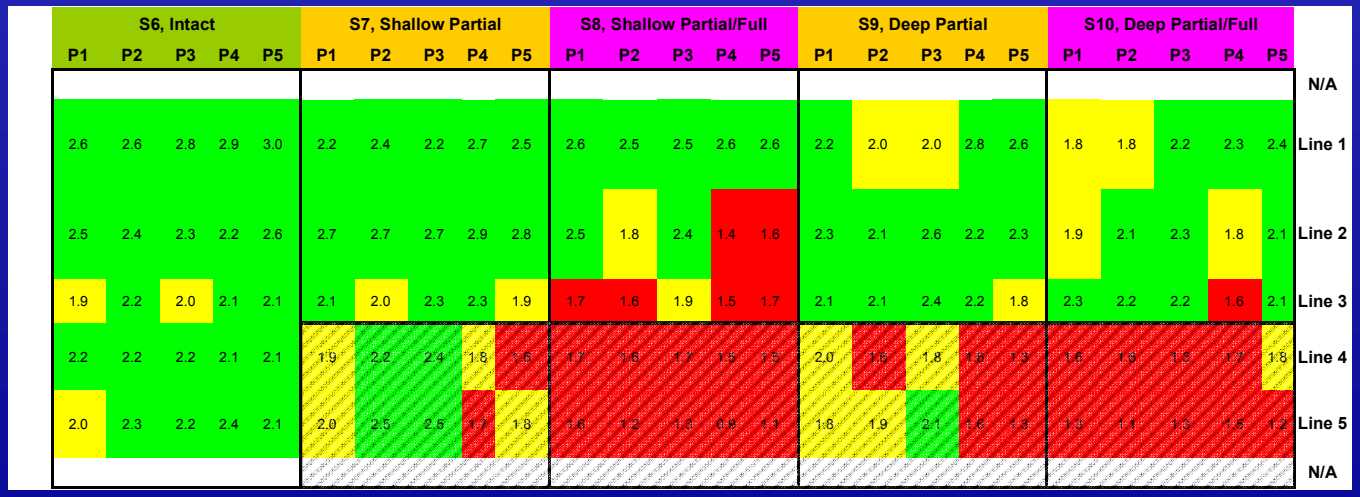

Average and standard deviation of control sections (1 and 6) used as reference

Infrared Results

Only the severely debonded area within the transition zone was clearly detected

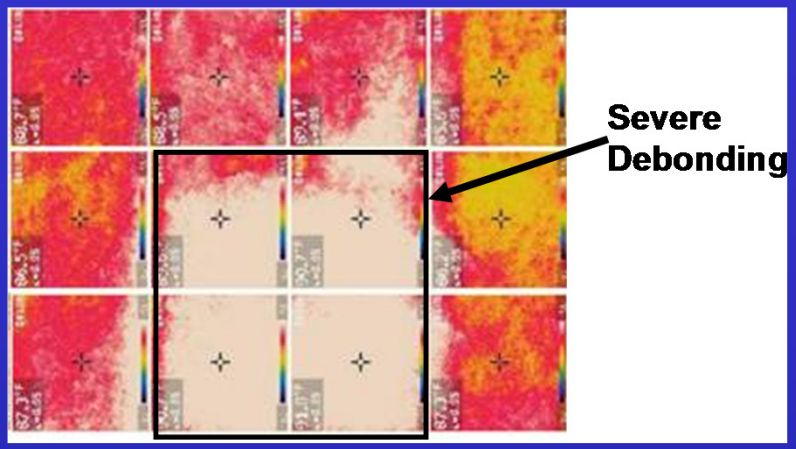

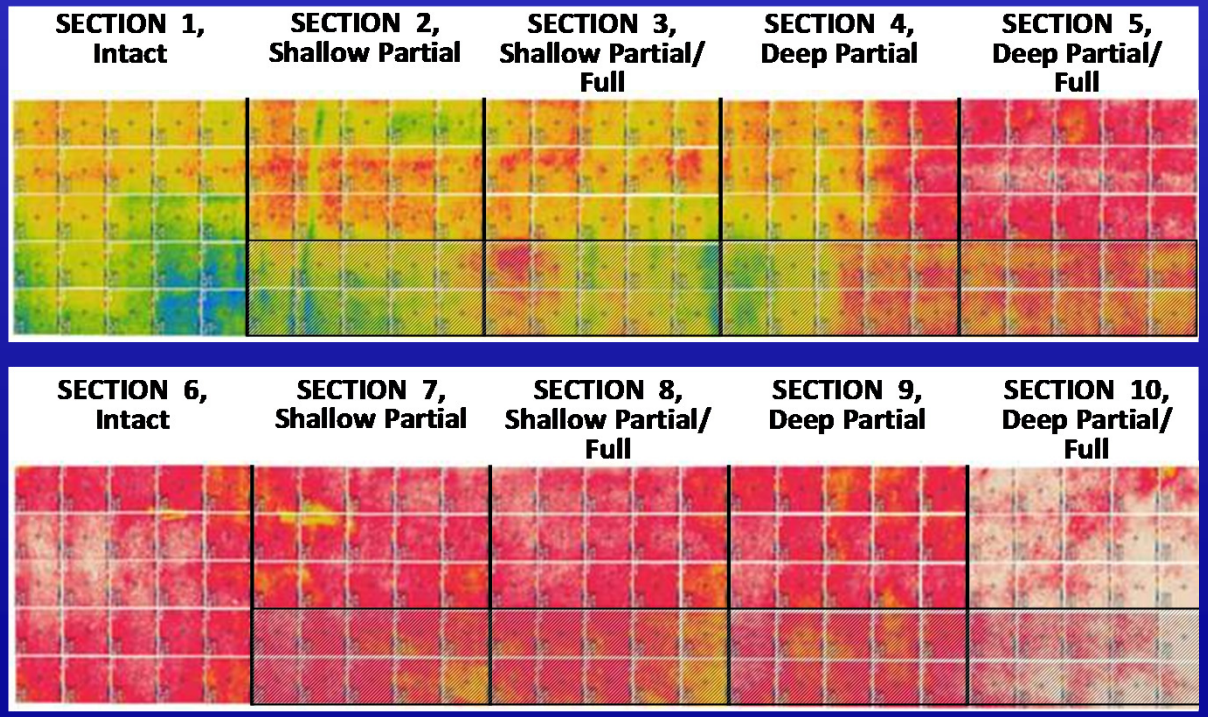

Passive source (sunlight) used to create the temperature differentials